An SIW Based Large-Scale Corporate-Feed Array Antenna

Dong-Fang Guan, Can Ding, Zu-Ping Qian, Ying-Song Zhang,
Wen-Quan Cao, and Eryk Dutkiewicz

Abstract—A 16×16 substrate integrated waveguide (SIW) cavity-backed array antenna is proposed in this paper. The array consists of two layers. The top layer employs novel SIW based sub-arrays with a compact size. The bottom layer is an 8×8 SIW corporate-feed network to feed the sub-arrays. The Chebyshev amplitude weighting is employed in the feed network, which substantially reduces the side lobe level. The array antenna is fabricated using low cost printed circuit board technology. The experimental results show that the proposed array antenna has a large bandwidth of 15% from 18.5 GHz to 21.5 GHz with a peak gain of 29.1 dBi at 20.5 GHz. Across the entire band, high radiation efficiency above 62% and a low side lobe level below -17 dB are realized. The design principle can be used as a guidance for large-scale planar array antenna design and the proposed antenna can be used as a receiving antenna located on the ground in satellite communication systems.

Index Terms—Antenna array, sub-array, substrate integrated waveguide, Chebyshev distribution, side lobe level, high gain, large bandwidth.

I. INTRODUCTION

L ARGE-SCALE planar array antenna is one of the most popular approaches to realize a high-gain pencil beam, and it has been extensively utilized in modern communications systems, such as satellite communications, remote sensing, radar systems, and relay networks. It has the advantages of a low profile and light weight compared with the other high gain antennas such as reflector array and horn antennas. There are several types of large-scale array antennas available in the literature. The most traditional ones are based on microstrip lines because of their low profile, compact size, low cost, and easy integration with various planar circuits [1]-[3]. However, conventional microstrip-feed networks suffer from high loss and may introduce spurious radiation, thereby leading to a high side lobe level (SLL) and low antenna efficiency. A metallic waveguide or hollow waveguide is a substitute with minor dielectric and radiation loss and can achieve high efficiency. Nevertheless, limited by the design complexity and high cost, it is not suitable for mass production [4]-[7].

A substrate integrated waveguide (SIW) is a more competitive candidate since it has both the advantages of the microstrip line and metallic waveguide, such as low loss, low cost and easy integration with planar circuits [8]-[9]. Generally, arrays based on the SIW structure can be divided into two groups: series-feed arrays [10]-[13] and cavity-backed arrays [14]-[19]. These arrays reported in the literature have excellent radiation performance but with significant disadvantages when expanding to large-scale arrays. The bandwidths of series-feed slot array antennas tend to decrease as the number of antenna elements increases. For example, the 16×16 slot array proposed in [13] has a bandwidth of only 2.7%. Meanwhile, corporate-feed SIW arrays have feed networks distributed around the radiating aperture which limits the scale of the array and degrades the antenna efficiency.

Recently, a few solutions have been proposed to design large-scale SIW based array antennas. In [20]-[22], low temperature co-fired ceramic (LTCC) technology was employed. The proposed array is able to expand freely since the corporate-feed network and the radiating elements are placed on different layers. However, LTCC has high design complexity and high cost. Hybrid array structures using SIW and microstrip lines have been introduced in [23]-[26] as a substitute solution. However, high loss and spurious radiation caused by microstrip lines are still unavoidable in these designs.

In our previous work [27], a 4×4 cavity-backed array was proposed without an individual feed network, resulting in a substantial size reduction. However, the array has a relatively narrow bandwidth for industrial applications such as satellite communications and the design principle only

D. F. Guan, Z. P. Qian, Y. S. Zhang, and W. Q. Cao are with the College of Communications Engineering, PLA University of Science and Technology, Nanjing 210007, China (e-mail:gdfguandongfang@163.com).

Y. S. Zhang is also with the State Key Laboratory of Millimeter Waves, Southeast University, Nanjing, China

C. Ding is under cotutelle arrangement between Macquarie University, Sydney, Australia, and Xidian University, Xi'an, Shanxi, China. He is also working with the DP&S Flagship of Commonwealth Scientific and Industrial Research Organization (CSIRO), Sydney, Australia (e-mail: can.ding@csiro.au).

Eryk Dutkiewicz is with the Department of Engineering, Macquarie University, Sydney, Australia.
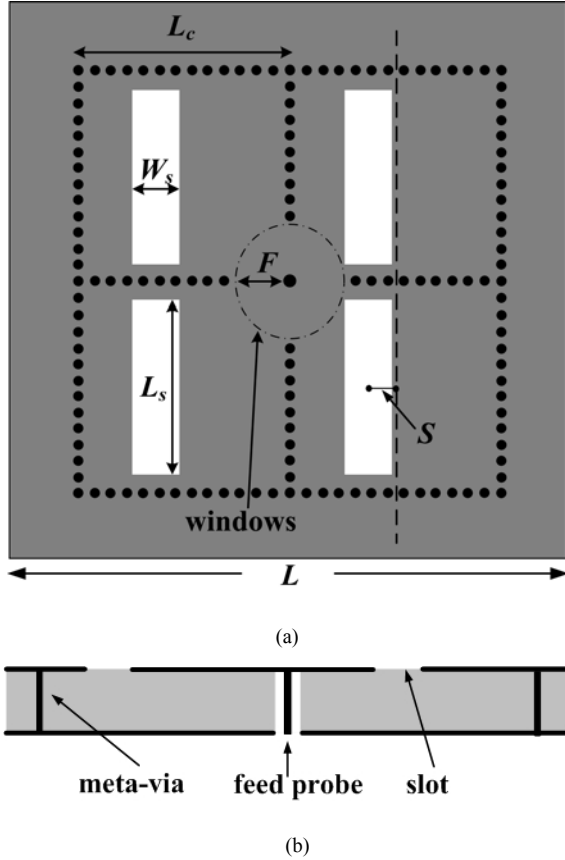
(a)

(b)

Fig. 1. (a) Top view and (b) side view of the 2×2 sub-array.

applies to arrays with a limited number of elements. In this work the array structure introduced in [27] is further studied and improved to achieve better performance. A new structure shown in Fig. 1(a) consisting of 2×2 radiating slots is advocated for its more compact size and doubled bandwidth of 15%, compared with the bandwidth of 6.7% in the previous work. Subsequently, it has been used as sub-arrays in constructing a larger-scaled pure SIW cavity-backed array. The array antenna consists of two layers. The top layer is occupied by 8×8 of the proposed sub-arrays. On the bottom layer, an 8×8 SIW Chebyshev distribution corporate-feed network is built to feed the sub-arrays. In this work, the array is designed as a receiving antenna on the ground for satellite communications with a commonly required band from 18.3 GHz to 21.2 GHz. The test results show that the array is able to cover this band and is suitable for mass production for its advantages of high gain, high efficiency, low SLL and low cost.

The paper is organized as follows. The architecture, theory, and measured results of the sub-array are presented in Section II. Section III describes the SIW based feed network with a Chebyshev amplitude distribution to feed 8×8 sub-arrays described in the previous section. In Section IV, a 16×16 antenna array is built by stacking the sub-array and feed network together and the measurement results are discussed. Finally, the paper is summarized in Section V.
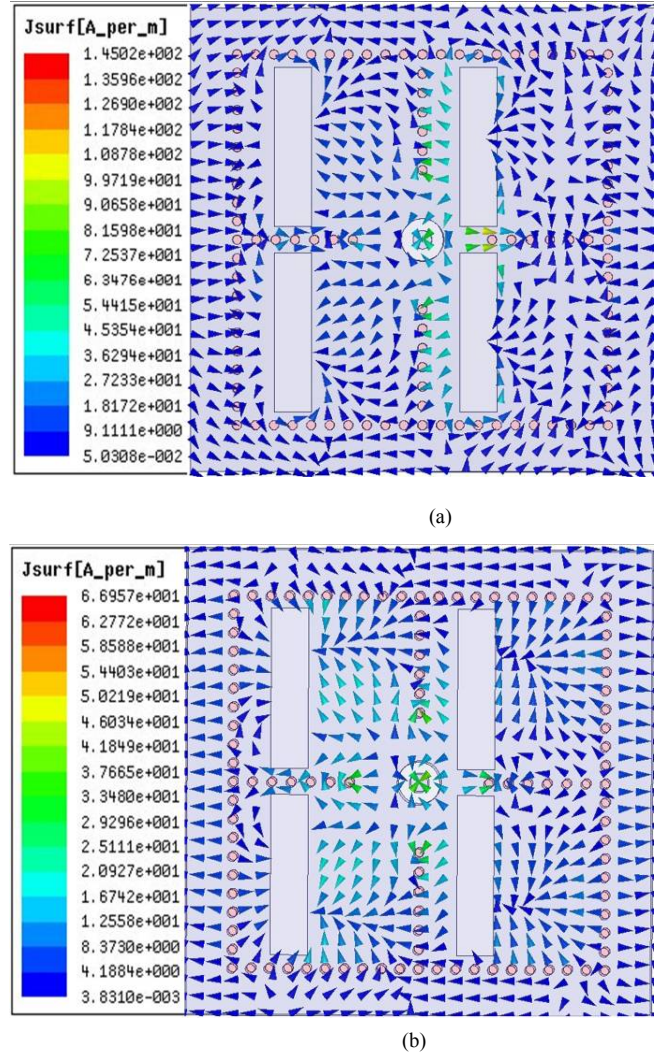

(a)

(b)

Fig. 2. Current distributions of the sub-array in (a) odd mode and (b) even mode.

II. 2×2 SUB-ARRAY DESIGN

Fig. 1(a) and 1(b) give the top and side views of the proposed sub-array, respectively. As shown in Fig. 1(a), the sub-array is composed of four square SIW cavities with the identical length of L_c. The cavities are point-to-point linked by inductive windows and fed by a feed probe located in the center of the windows. Due to the symmetric conducting windows, the energy can be split into four cavities equally without any feed networks. Rectangular slots with the size of $L_s \times W_s$ are etched on the top surface of each cavity so that the energy can radiate out. The sub-array is constructed on a Rogers-Duroid 5880 substrate with a dielectric constant of ε_r =2.2, a loss tangent of $tan\delta$ = 0.0009 and a substrate thickness of h = 1.5 mm.

To achieve a boresight radiation beam with high gain performance, identical or similar in-phase current distributions on the four slots are required, so that the radiation can add up at the boresight direction. When the slots are placed at the center of the cavities, the currents on the left-hand and right-hand

L_c	L_s	W_s	F	S
10.0	8.6	2.0	3.8	2.2

TABLE II
COEFFICIENT MATRIX OF 8×8 CHEBYSHEV DISTRIBUTIONS

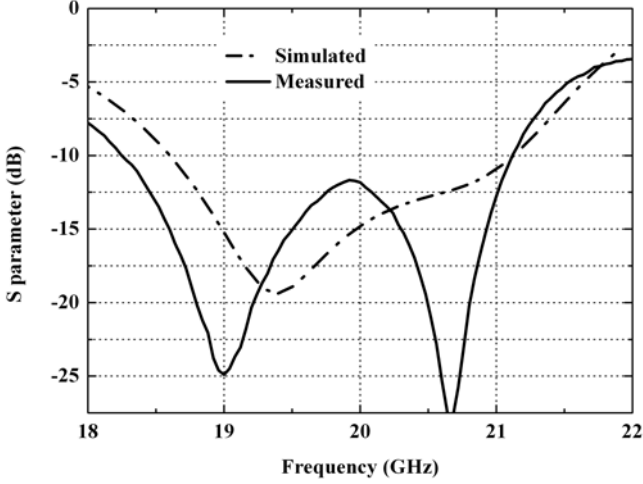|	A_{i1}	A_{i2}	A_{i3}	A_{i4}	A_{i5}	A_{i6}	A_{i7}	A_{i8}
A_{1j}	1	1.7	2.6	3.1	3.1	2.6	1.7	1
A_{2j}	1.7	1.87	4.42	5.27	5.27	4.42	1.87	1.7
A_{3j}	2.6	4.42	6.76	8.06	8.06	6.76	4.42	2.6
A_{4j}	3.1	5.27	8.06	9.61	9.61	8.06	5.27	3.1
A_{5j}	3.1	5.27	8.06	9.61	9.61	8.06	5.27	3.1
A_{6j}	2.6	4.42	6.76	8.06	8.06	6.76	4.42	2.6
A_{7j}	1.7	1.87	4.42	5.27	5.27	4.42	1.87	1.7
A_{8j}	1	1.7	2.6	3.1	3.1	2.6	1.7	1

Fig. 3. Simulated and measured reflection coefficients (S_{11}) of the sub-array.

Fig. 4. Simulated and measured gains of the sub-array.

shows the current distribution at the second resonant point. It is noted that although the current flow directions are inverse at the two sides of the slots, the currents toward the left are apparently stronger than those toward the right for all the slots. The resultant radiation of the slots is still in phase in this mode. Since the in-phase radiation of the 2×2 radiating elements can be obtained in both of the modes, the bandwidth enhancement is realized by merging the two modes together.

The dimension values of the sub-array are optimized by using the full wave software HFSS within the overall consideration and presented in Table I. The design and optimization procedures are as follows. First of all, the length of the radiating slot L_s is chosen since it determines the center working frequency. Subsequently, the width of the cavities L_c should be only slightly larger than L_s to guarantee a small aperture size. Meanwhile, L_c is the separation distance between the radiating elements in the array design and should be $\lambda_0/2 \leq L_c \leq \lambda_0$, where λ_0 is the wavelength in free space. Then, S is optimized to activate both the odd and even modes described in the previous paragraph. Finally, the width of the conductive windows F is tuned to achieve a good impedance match. In addition, the slot width W_s also has some slight influence on the bandwidth.

Fig. 3 gives the simulated and measured reflection coefficients of the proposed sub-array. According to the simulated S_{11}, the sub-array has two resonant points at 19.4 GHz and 21 GHz, respectively. Although it is not very distinct in the simulated results, the two resonant points at 19 GHz and 20.6 GHz are clearly observed in the measured results. Fig. 4 shows the simulated and measured gains of the array at the boresight. It is observed in the figure that the measured gain of the sub-array is above 11.5 dBi from 18.5 GHz to 21.5 GHz, with the peak gain of 12.9 dBi at 20 GHz. The gain variation of the sub-array is due to the phase mismatch of the currents on the four slots as the working frequency shifts away from the centre frequency (20 GHz). With the advantages of a high gain, a large bandwidth (15%) and a compact structure without an extra feed network, the proposed sub-array is an outstanding candidate for high-gain planar arrays.
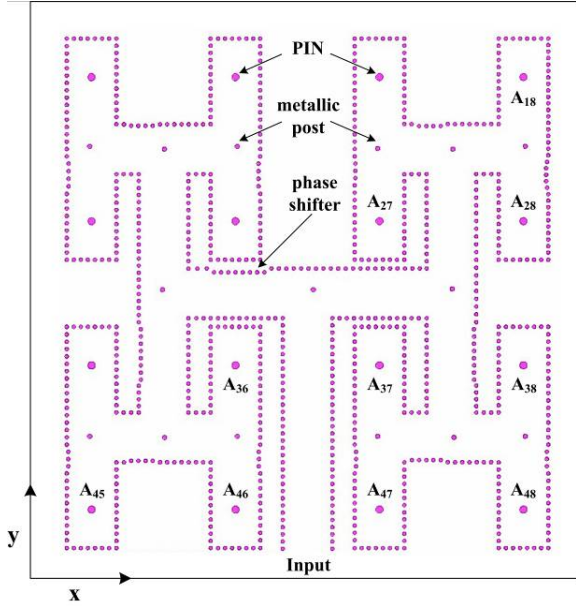
sides' slots are out of phase. It is found that the phase match on the slots can be obtained by moving the slots away from the symmetry axis of the SIW cavities. Furthermore, by tuning the translating parameter S, two resonant points can be introduced to increase the bandwidth. The operating mechanism can be analyzed using the even-odd mode theory. Fig. 2(a) and 2(b) depict the current distributions on the sub-array obtained from Ansoft HFSS in the odd and even modes, respectively. In the odd-mode as shown in Fig. 2(a), the directions of the current flow at the two sides of each slot are identical. This demonstrates that the equivalent displacement currents on the four slots are in phase. Therefore, the energy radiated by the slots adds up in this mode. Fig. 2(b)

Fig. 5. Configuration of 1/4 feed network in the first quadrant.

TABLE III
S PARAMEPERS EQUIVALENT TO CHEBYSHEV AMPLITUDE
COEFFICIENTS

A_{45}	A_{46}	A_{36}	A_{47}	A_{37}
-8.6 dB	-9.4 dB	-10.1 dB	-11.2 dB	-12.0 dB
A_{48}	A_{38}	A_{27}	A_{28}	A_{18}
-13.5 dB	-14.3 dB	-15.7 dB	-16.1 dB	-18.4 dB

III. FEED NETWORK DESIGN

This section describes an 8×8 SIW feed network for the 16×16 planar array which consists of 64 sub-arrays designed in Section II. The feed network is built on a separate layer using Rogers-Duroid 5880 with a thickness of h=0.5 mm. The feed network is placed below the antenna layer to feed the sub-arrays. The prototype of the feed network is shown in Fig. 5. Due to the symmetric configuration of the feed network, only one fourth of the feed network (4×4) is presented to save space.

It is well known that SLL increases with the expansion of the array. To suppress the side lobe, a Chebyshev amplitude weighting method is employed in the feed network. The amplitude coefficients for the 8×8 outputs of the feed network are given in Table II. The coefficient matrix shown in the table can be divided into four quadrants. Since the coefficients in each quadrant are identical, only the coefficients in the first quadrant are mapped to the 1/4 feed network in Fig. 5.

As shown in Fig. 5, the feed network is made by cascading several T-junctions serving as 1-to-2 power dividers. Metallic posts are inserted in each T-junction to achieve an impedance match and to control the power ratio of the two outputs. When the metallic post is placed in the middle of the T-junction, the two output ports can have even amplitudes. If the metallic post
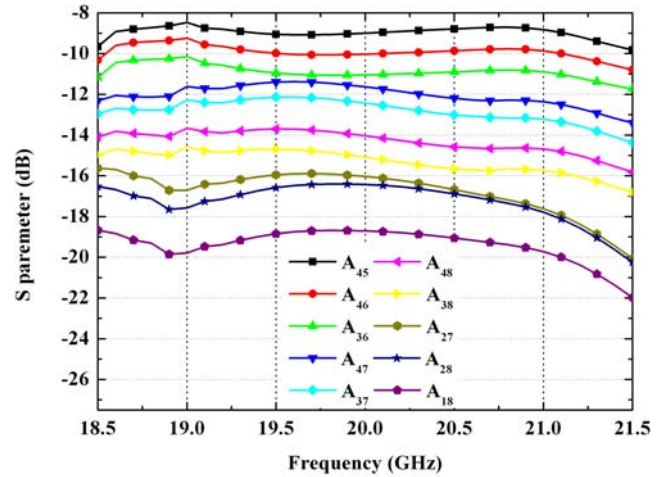

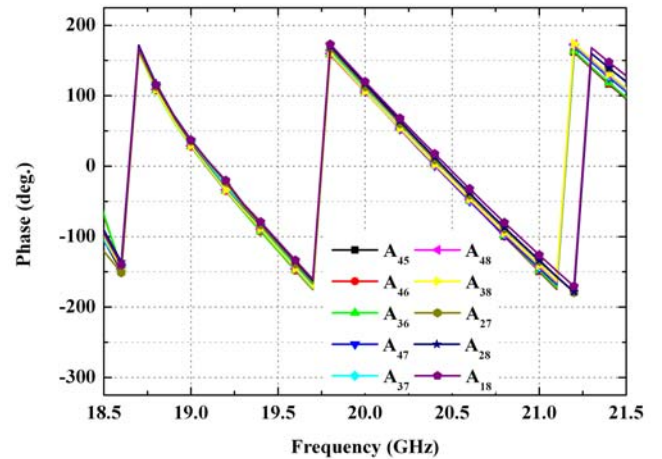Fig. 6. Simulated results of the amplitudes at the outputs of the feed network.

Fig. 7. Simulated results of the phases at the outputs of the feed network.

is shifted away from the middle point, non-uniform amplitudes of the two output ports can be obtained. Given a specific power ratio, the position of the metallic post can be easily determined with the help of HFSS or other simulation software. The power ratios of the power dividers can be calculated according to the required amplitude values listed in Table II.

It is to be noted that phase shifts between the two outputs of a power divider are introduced when the metallic post is shifted away from the center. Phase shifts can be compensated by altering the widths of the SIW at the output ports. The SIW with different widths shown in Fig. 5 can be seen as built-in phase shifters. The theory and detailed design method was studied in [28]. In this work, each power divider (T-junction) in the feed network is designed separately to achieve a Chebyshev amplitude distribution with identical phases. The repetitive design details are not presented in this paper.
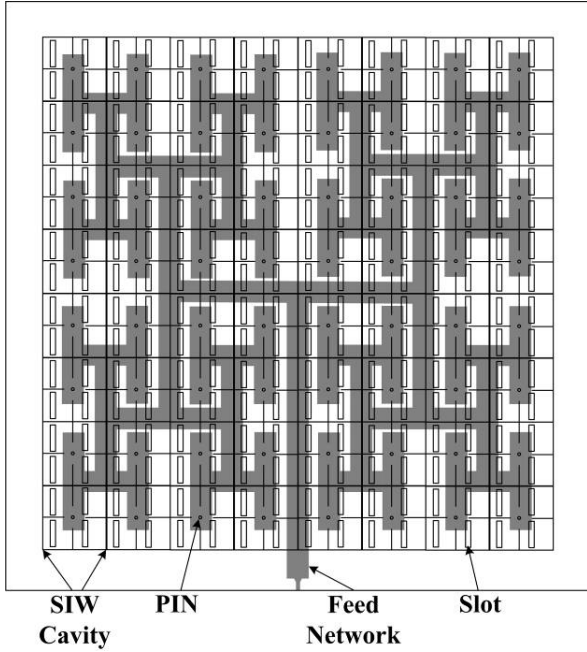
Fig. 8. Configuration of the 16×16 array.

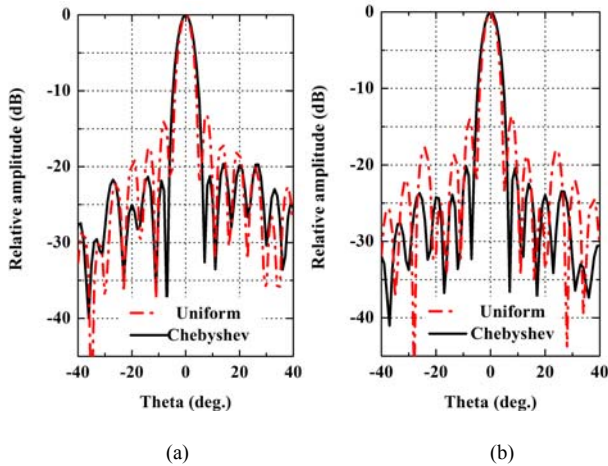(a)   (b)

Fig. 9. Radiation patterns of the array with the Chebyshev and uniform feed networks in (a) E-plane and (b) H-plane at 20 GHz.

Figs. 6 and 7 show the simulated transmission coefficients of the feed network. Although the 1/4 feed network shown in Fig. 5 has 16 output ports (PINs), there are only 10 different Chebyshev amplitude values of the output ports according to Table II. Therefore, only 10 curves of the transmission coefficients are presented in Figs. 6 and 7 to avoid repetition. For the sake of comparison, coefficient values in the first quadrant of Table II have been redefined in dB and presented in Table III. The amplitude curves plotted in Fig. 6 are generally in accordance with the theoretical data shown in Table II. The minor discrepancies between the simulated results and the theoretical values are attributed to the dielectric loss in the substrate. As observed in Fig. 7, the current phases at the outputs of the feed network are identical. It is thus deduced that an in-phase Cheybysheve amplitude distribution is achieved by using the feed network described in Fig. 5.
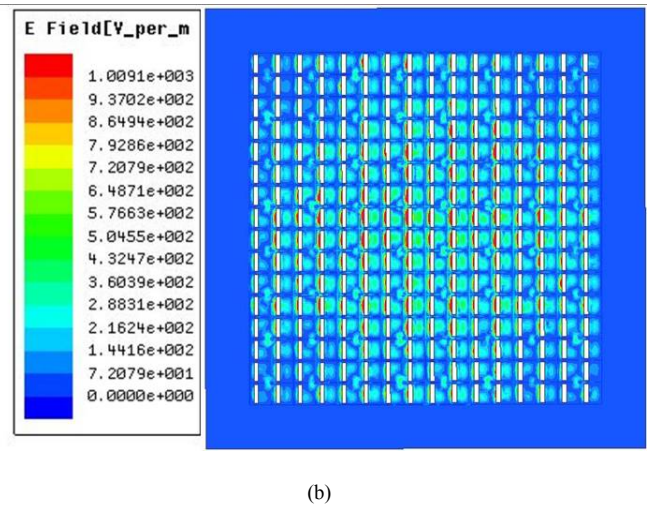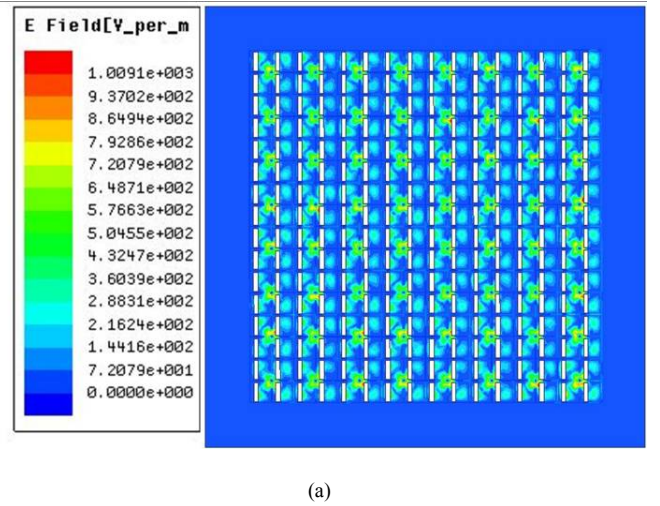

(a)

(b)

Fig. 10. E-field distributions on the array with (a) uniform amplitude distribution, and (b) Chebyshev amplitude distribution feed.

IV. 16×16 ARRAY DESIGN

A. Side Lobe Suppression Assessment

A 16×16-elements planar array antenna is constructed by stacking the sub-arrays described in Section II on the top of the feed network presented in Section III. Fig. 8 shows the configuration of the array in the perspective view. The gray area represents the SIW corporate-feed network on the bottom layer. It is a six-level power divider network consisting of several SIW T-junctions. The tiny rectangles are the radiating slots on the top layer. Metallic PINs are inserted in both of the layers to stitch them up.

The simulated E- and H-planes far-field radiation patterns at the center frequency (20 GHz) of the array antenna are presented in Fig. 9. To illustrate the SLL improvement by using the feed network with a Chebyshev amplitude distribution, simulated radiation patterns of the array with a uniform amplitude distribution are also depicted in the figure. It is observed that the SLL of the array employing
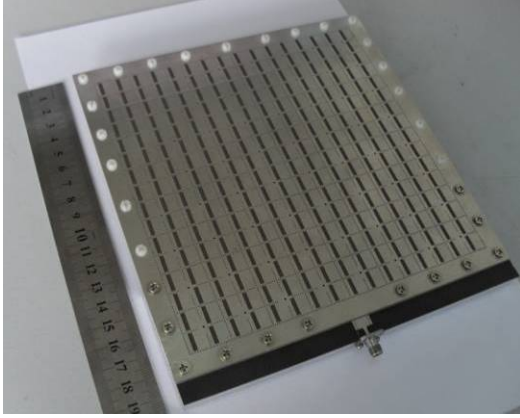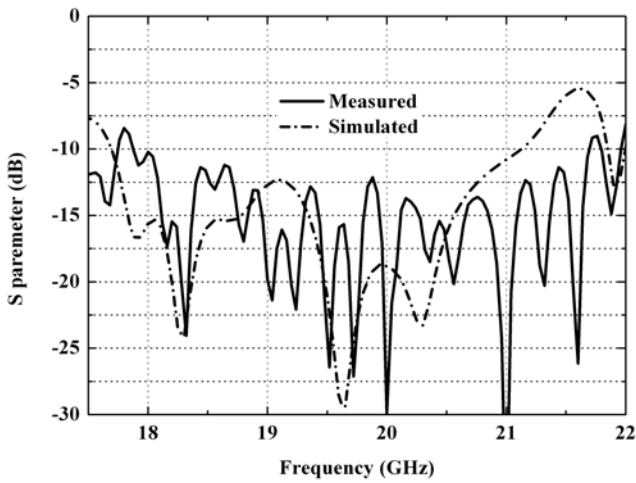
Fig. 11. Photograph of the fabricated array.

Fig. 12. Simulated and measured reflection coefficients (S_{11}) of the array.

Chebyshev amplitude distribution is significantly reduced compared to that with a uniform amplitude distribution. In addition, the E-field distributions on the array with both Chebyshev and uniform amplitude feed networks at 20 GHz are illustrated in Fig. 10.

B. Measured Results of the 16×16 Array

As shown in Fig. 11, the proposed 16×16 SIW backed-cavity planar antenna array has also been fabricated and tested for verification. It has an array size of 180×190 mm^2 and an aperture size of 160×160 mm^2. The printed circuit board (PCB) technology is employed in the fabrication process which is low cost and suitable for mass production. The positions of the vias on the two layers are designed for ease of alignment. Therefore, the two layers of the antenna can be aligned and fixed by screws. The simulated and measured reflection coefficients of the array antenna are depicted in Fig. 12. As shown in the figure, there exist some ripples in the measured S_{11} which are mainly attributed to the reflections between the feed network and the top layer. The ripples can be eliminated by employing more screws and customized

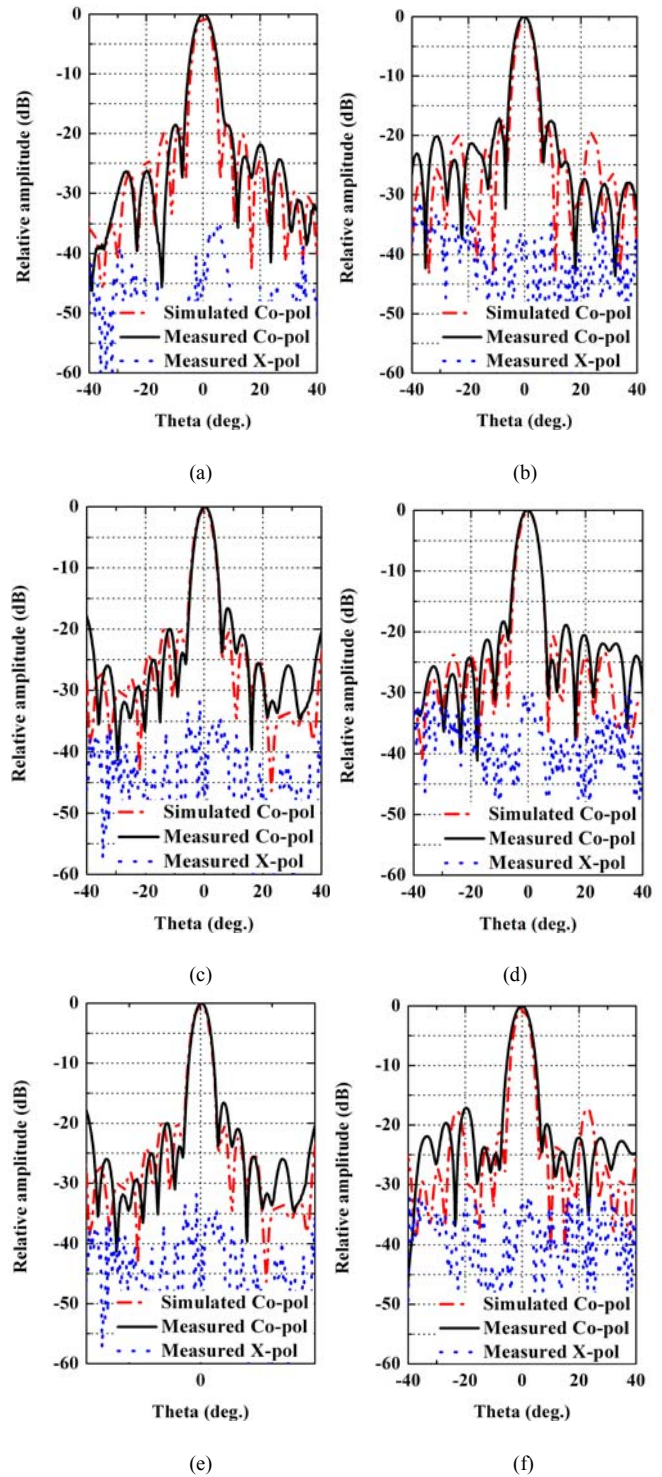Fig. 13. Simulated and measured normalized radiation patterns in (a) E-plane at 19 GHz, (b) H-plane at 19 GHz, (c) E-plane at 20 GHz, (d) H-plane at 20 GHz, (e) E-plane at 21 GHz, (f) H-plane at 21 GHz.

PINs or by using other advanced bonding technology to achieve a better alignment. According to the measured results, the array antenna has a -10 dB impedance bandwidth of 19.2% from 17.9 GHz to 21.7 GHz.

TABLE IV

COMPARISON BETWEEN DIFFERENT LARGE-SCALE PLANAR ARRAY ANTENNAS

	f_0 (GHz)	No. of Element	No. of Layer	Size (λ_0)	Band Width (%)	Gain (dBi)	First SLL (dB)	Radiation Efficiency (%)	Aperture Efficiency (%)	Type
[1]	60	50	1	7×7×0.05	12.5	25.2	-9	63.7	53.8	Microstrip (PCB)
[7]	60	256	2	15.4×15.6×0.6	8.3	33	-12.3	83.6	66.1	Hollow-waveguide
[20]	60	64	20	9.4×6.2×0.4	17.1	22.1	-13	44.4	22.1	SIW (LTCC)
[23]	12.5	64	2	6.3×6.3×0.08	13	24	-12	N/A	50	SIW and Microstrip (PCB)
[25]	94	1024	2	28.8×20.7×0.3	6.4	29.9	-9	24	13.1	SIW and Microstrip (PCB)
Our work	20	256	2	12×12.6×0.13	15	29.1	-17	76	42.8	SIW (PCB)

The aperture efficiency is calculated using (Measured Gain)/(Max Theoretical Gain) and the maximum theoretical gain is 4*pi*A/lambda^2, where A is the physical aperture area.
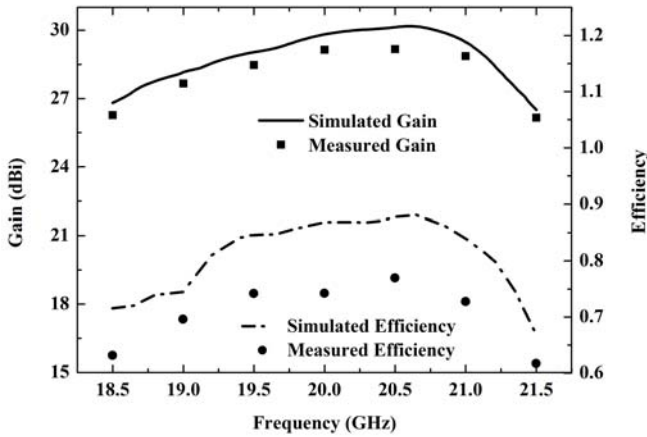

Fig. 14. Simulated and measured gains and radiation efficiencies of the array.

The gain and radiation patterns of the array are measured in a chamber with a far-field setup. The gain values are obtained by comparing the received current density on the tested antenna against that on a standard gain horn antenna. The system error of this measurement system on the gain is less than 0.5 dB. Figs. 13(a-f) show the simulated and measured radiation patterns in the E- and H-planes at 19, 20 and 21 GHz, respectively.

As shown in Fig. 13, the 3-dB beamwidths in both the E- and H-planes are 5°. The measured SLL and cross-polarization levels are below -17 dB and -30 dB, respectively, across the entire work band. Fig. 14 shows the simulated and measured gains and radiation efficiencies. The measured gains agree quite well with the simulated results with a maximum discrepancy of 1 dB and the peak gain can reach up to 29.1 dBi at 20.5 GHz. It is also noted that the 3-dB gain bandwidth is from 18.5 GHz to 21.5 GHz and is inside the range of the

impedance bandwidth. Consequently, the actual work bandwidth of the array is 15% from 18.5 GHz to 21.5 GHz. The radiation efficiency can be as high as 76% at 20.5 GHz and is above 62% within the entire band. The variations of the array efficiency and gain with the frequency are attributed to the fact that the gain variation of the sub-array is amplified as several sub-arrays are employed. The maximum aperture efficiency is calculated to be 42.8% using the measured gain and aperture size. The relatively low value is caused by the excessive losses in the large feed network.

Detailed comparisons between some representative works mentioned in Section I and this work are illustrated in Table IV. The SIW based planar array proposed in our design has four merits compared to other corporate-feed ones listed in the table. Firstly, the proposed array antenna has a superior bandwidth of 15%. This is attributed to the broadband characteristics of both the sub-array and the corporate-feed structure. Secondly, low SLL of the array is achieved. Moreover, with the Chebyshev amplitude distribution feed network, low SLL can always be guaranteed for larger arrays with more elements. Thirdly, the array has high radiation efficiency, which is 76% at 20.5 GHz. This is due to the fact that both the feed network and the radiating elements are designed using a closed SIW structure. Although the array employing a hollow waveguide in [7] can realize a slightly higher efficiency, it has half the bandwidth, higher SLL and design complexity. Fourthly, the antenna array is fabricated using the PCB process which is low cost and suitable for mass production.

V. CONCLUSION

A 16×16 SIW cavity-backed array antenna was proposed in this paper. It has two layers where the radiation elements and

the feed network are placed on the top and bottom layers, respectively. A novel broadband SIW sub-array structure without an extra feed network has been proposed, leading to the compact size of the final array. The feed network is also constructed using the SIW technology. It is very easy for the SIW based power divider to control the amplitudes and phases of the output ports. A substantial reduction in the SLL has been achieved by manipulating the dimensions of the feed network to realize a Chebyshev amplitude distribution. The final array was fabricated using the PCB technology with low cost. The measured results of the fabricated array antenna have been compared with comparable works in the literature, demonstrating excellent enhancements in the antenna performance, such as a broad bandwidth, high efficiency, low SLL and low cost. The realized antenna can be used as the receiving antenna for space to earth communications. The proposed design principle can be used as a guidance to design SIW based large-scale planar arrays in the future.

REFERENCES

[1] M. J. Li, and K. M. Luk, "A low-profile unidirectional printed antenna for millimeter-wave applications," *IEEE Trans. Antennas Propag.*, vol. 62, no. 3, pp. 1232–1237, Mar. 2014.

[2] B. Zhang and Y. P. Zhang, "Grid array antennas with subarrays and multiple feeds for 60-GHz radios," *IEEE Trans. Antennas Propag.*, vol. 60, no. 5, pp. 2270–2275, May 2012.

[3] E. Levine, G. Malamud, S. Shtrikman, and D. Treves, "A study of microstrip array antennas with the feed network," *IEEE Trans. Antennas Propag.*, vol. 37, no. 4, pp. 426–434, Apr. 1989.

[4] D. Kim, J. Hirokawa, M. Ando, J. Takeuchi and A. Hirata, "64×64-element and 32×32-element slot array antennas using double-layer hollow-waveguide corporate-feed in the 120 GHz band," *IEEE Trans. Antennas Propag.*, vol. 62, no. 3, pp. 1507–1512, Mar. 2014.

[5] T. Tomura, Y. Miura, M. Zhang, J. Hirokawa and M. Ando, "A 45° linearly polarized hollow-waveguide corporate-feed slot array antenna in the 60-GHz band," *IEEE Trans. Antennas Propag.*, vol. 60, no. 8, pp. 3640–3646, Aug. 2012.

[6] M. Zhang, J. Hirokawa, and M. Ando, "An E-band partially corporate feed uniform slot array with laminated quasi double-layer waveguide and virtual PMC terminations," *IEEE Trans. Antennas Propag.*, vol. 59, no. 5, pp. 1521-1527, May 2011.

[7] Y. Miura, J. Hirokaw, M. Ando, Y. Shibuya, and G. Yoshida, "Double-layer full-corporate-feed hollow waveguide slot array antenna in the 60-GHz band," *IEEE Trans. Antennas Propag.*, vol. 59, no. 8, pp. 2844–2851, Aug. 2011.

[8] W. Hong, K. Wu, H. J. Tang, J. X. Chen, P. Chen, Y. J Cheng, and J. F. Xu, "SIW-like guided wave structures and applications," *IEICE Trans. Electron.*, vol. E92-C, no. 9, pp. 1111–1123, Sep. 2009.

[9] K. Wu, D. Deslandes, and Y. Cassivi, "The substrate integrated circuits—a new concept for high-frequency electronics and optoelectronics," *Proc. 6th Int. Conf. Telecommunications Modern Satellite, Cable Broadcasting Service (TELSIKS'03)*, vol. 1, pp. P-III-P-X, Oct. 1–3, 2003.

[10] Y. Ding, and K. Wu, "A 4×4 ridge substrate integrated waveguide (RSIW) slot array antenna," *IEEE Antennas Wirel. Propag. Lett.*, vol. 8, pp. 561–564, 2009.

[11] Y. J. Cheng, W. Hong, and K. Wu, "94 GHz substrate integrated monopulse antenna array," *IEEE Trans. Antennas Propag.*, vol. 60, no. 1, pp. 121–129, Jan. 2012.

[12] X. P. Chen, K. Wu, L. Han, and F. F. He, "Low-cost high gain planar antenna array for 60-GHz band applications," *IEEE Trans. Antennas Propag.*, vol. 58, no. 6, pp. 2126–2129, Jun. 2010.

[13] J. F. Xu, W. Hong, P. Chen, and K. Wu, "Design and implementation of low sidelobe substrate integrated waveguide longitudinal slot array antennas," *IET Microw. Antennas Propag.*, vol. 3, no. 5, pp. 790–797, 2009.

[14] K. Gong, Z. N. Chen, X. M. Qing, Z. Song, P. Chen, and W. Hong, "Empirical formula of cavity dominant mode frequency for 60-GHz cavity-backed wide slot antenna," *IEEE Trans. Antennas Propag.*, vol. 61, no. 2, pp. 969–972, Feb. 2013.

[15] K. Gong, Z. N. Chen, X. M. Qing, Z. Song, P. Chen, and W. Hong, "Substrate integrated waveguide cavity-backed wide slot antenna for 60-GHz bands," *IEEE Trans. Antennas Propag.*, vol. 60, no. 12, pp. 6023–6026, Dec. 2012.

[16] Y. Zhang, Z. N. Chen, X. M. Qing, and W. Hong, "Wideband millimeter-wave substrate integrated waveguide slotted narrow-wall fed cavity antennas," *IEEE Trans. Antennas Propag.*, vol. 59, no. 5, pp. 1488–1496, May 2011.

[17] T. Mikulasek, A. Georgiadis, A. Collado, and J. Lacik, "2×2 microstrip patch antenna array fed by substrate integrated waveguide for radar applications," *IEEE Antennas Wireless Propag. Lett.*, vol. 12, pp. 1287–1290, 2013.

[18] T. Y. Yang, W. Hong and Y. Zhang, "Wideband millimeter-wave substrate integrated waveguide cavity-backed rectangular patch antenna," *IEEE Antennas Wirel. Propag. Lett.*, vol. 13, pp. 205–208, 2014.

[19] Eun-Young Jung, Jae W. Lee, Taek K. Lee, and Woo-Kyung Lee, "SIW-based array antennas with sequential feeding for X-band satellite communication," *IEEE Trans. Antennas Propag.*, vol. 60, no. 8, pp. 3632-3638, August 2012.

[20] J. F. Xu, Z. N. Chen, X. M. Qing, and W. Hong, "Bandwidth enhancement for a 60 GHz substrate integrated waveguide fed cavity array antenna on LTCC," *IEEE Trans. Antennas Propag.*, vol. 59, no. 3, pp. 826–832, Mar. 2011.

[21] J. F. Xu, Z. N. Chen, X. M. Qing, and W. Hong, "140-GHz planar broadband LTCC SIW slot antenna array," *IEEE Trans. Antennas Propag.*, vol. 60, no. 6, pp. 3025–3028, Jun. 2012.

[22] J. F. Xu, Z. N. Chen, X. M. Qing, and W. Hong, "140-GHz TE20-mode dielectric-loaded SIW slot antenna array in LTCC," *IEEE Trans. Antennas Propag.*, vol. 61, no. 4, pp. 1784–1793, Apr. 2013.

[23] M. H. Awida, S. H. Suleiman, and Aly E. Fathy, "Substrate-integrated cavity-backed patch arrays: a low-cost approach for bandwidth enhancement," *IEEE Trans. Antennas Propag.*, vol. 59, no. 4, pp. 1155–1163, Apr. 2011.

[24] M. H. Awida, and Aly E. Fathy, "Substrate-integrated waveguide Ku-band cavity-backed 2×2 microstrip patch array antenna," *IEEE Antennas Wireless Propag. Lett.*, vol. 8, pp. 1054–1056, 2009.

[25] Y. J. Cheng, Y. X. Guo, and Z. G. Liu, "W-Band Large-Scale High-Gain Planar Integrated Antenna Array," *IEEE Trans. Antennas Propag.*, vol. 62, no. 6, pp. 3370–3373, Jun. 2014.

[26] A. Borji, D. Busuioc, and S. Safavi-Naeini, "Efficient, low-cost integrated waveguide-fed planar antenna array for Ku-band applications," *IEEE Antennas Wirel. Propag. Lett.*, vol. 8, pp. 336-339, 2009.

[27] D. F. Guan, Z. P. Qian, Y. S. Zhang, and Y. Cai, "Novel SIW cavity-backed antenna array without using individual feeding network," *IEEE Antennas Wirel. Propag. Lett.*, vol. 13, pp. 423-426, 2014.

[28] Y. J. Cheng, W. Hong, and K. Wu, "Novel substrate integrated waveguide fixed phase shifter for 180-degree directional coupler," *IEEE MTT-S Int. Microw. Symp. Dig.*, Honolulu, HI, Jun. 2007, pp. 189–192.